

Manuscript Details

Manuscript number	PROOCE_2017_45
Title	Conditions for assessing zooplankton abundance with LOPC in coastal waters.
Article type	Full Length Article

Abstract

Recent technical advances in laser-based systems to measure zooplankton distribution have opened new perspectives in ecological and behavioral studies by improving significantly the horizontal and vertical sampling resolution, providing information on zooplankton patchiness and on the influence of small scale physical processes. The application of laser-based systems also led to new challenges on the identification of organisms vs. particulate matter. In areas with high detritus abundances zooplankton abundances might be overestimated by counting plankton and detritus together. We investigated the contribution of detritus in Laser Optical Plankton Counter (LOPC) data collected during two cruises on the continental shelf of the Gulf of Lion (NW Mediterranean Sea). The study area is characterized by several types of ecoregions owing to the influence of winds, freshwater run off and intrusion of oligotrophic waters from offshore. We identified the main mechanisms leading to the formation of detritus as a function of environmental conditions and developed a method to assess the contribution of detritus in LOPC counts based on the proportion of large particles (multi-element plankton, MEPs). Highest percentages of detritus were found in stratified conditions associated with high chl-a concentration (up to 90 % of the counts). Discontinuities in density profiles alone also resulted in peaks of particles concentrations. We suggest a threshold of 2 % of MEPs in LOPC counts above which the LOPC is most likely counting more detritus than organisms. This easy check of the detritus contribution to total LOPC counts was applied to datasets from different marine ecological situations (glacial input, clear water, productive shelf) and proved valid in different biogeographical regions (e.g. high latitude and tropical habitats).

Keywords	laser-based sensors; ZooScan; stratification; thin layers; aggregates
Manuscript category	Biological Oceanography
Corresponding Author	Boris Espinasse
Corresponding Author's Institution	University of British Columbia
Order of Authors	Boris Espinasse, Sünnje Basedow, Sabine Schultes, Meng Zhou, Leo Berline, Francois Carlotti
Suggested reviewers	Kohei Matsuno, Pieter Vandromme, Marc Hufnagl, Jason Everett

Submission Files Included in this PDF

File Name [File Type]

cover letter.docx [Cover Letter]

LOPC-ms-new-15-02.docx [Manuscript]

Fig_LOPC_new.docx [Figure]

Tables.docx [Table]

Highlights.docx [Highlights]

To view all the submission files, including those not included in the PDF, click on the manuscript title on your EVISE Homepage, then click 'Download zip file'.



University of British Columbia
Department of Earth, Ocean, and Atmospheric Sciences,
2207 Main Mall, Vancouver,
British Columbia, Canada V6T 1Z4

Tel: + 778 316 6640
Email: boris.espinasse@laposte.net

February 15, 2017

Dear Guest Editor,

On the behalf of all coauthors, I am submitting this manuscript entitled “**Conditions for assessing zooplankton abundance with LOPC in coastal waters**” for your consideration to be published in *Progress in Oceanography* (in the Mermex special issue) as an original research article.

This study deals with the use of laser-based sensors in coastal waters and our need to understand better the information obtained from these systems. We highlighted the role of different types of environmental conditions in the formation of detritus and we developed thresholds based on indicators derived from Laser Optical Plankton Counter data that can be used to estimate the contribution of detritus in total counts. The method was applied to other datasets from around the globe and proved valid.

A previous version of the manuscript was submitted in L&O: Methods (May 2016) and was rejected with possibility of a resubmission. Significant efforts were done to improve the manuscript since. Major changes were done on the text, tables and figures, and new datasets were included to test the method in other habitats. We think that the research theme and results should be well fitted for *Progress in Oceanography*.

All the co-authors have been working with the LOPC in the last ten years and published several papers using LOPC data. They all shared their experience to make this study relevant and approved the submitted version of the ms. They contributed to improve the manuscript to its final version by correcting the language, providing comments and polishing the paper.

In addition to that and more specifically:

François Carlotti was the chief scientist during the research cruises and was involved in the two ANRs funding the cruises and the purchase of the LOPC and other optical sensors. He participated actively in the structuring of the paper.

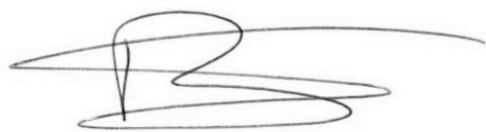
Meng Zhou joined the cruises, helping actively to collect and analyze the data. He was included in the ANR permitting the purchase of the instruments and gave valuable comments on an earlier version of the manuscript.

Sabine Schultes helped to structure the paper and has provided data allowing to validate the method in other areas.

Sünnje Basedow helped to develop the statistical aspect of the method (GAM) and gave comments on an earlier draft of the manuscript. She also provided data to validate the method in other areas.

Léo Berline helped to make the new version of the paper clearer and shared his experience concerning the use of other optical sensors.

Sincerely yours,

A handwritten signature in black ink, appearing to be 'Boris Espinasse', written in a cursive style with a long horizontal stroke extending to the right.

Dr. Boris Espinasse

Suggested Reviewers

Dr. Pieter Vandromme: pvandromme@geomar.de

Dr. Jason Everett: jason.everett@unsw.edu.au

Dr. Marc Hufnagl: marc.hufnagl@uni-hamburg.de

Dr. Kohei Matsuno: kohei.matsuno@utas.edu.au

1 **Conditions for assessing zooplankton abundance with LOPC in coastal waters.**

2
3
4 Authors:

5 Espinasse B.^{*, 1, 2, 3}, Basedow S.⁴, Schultes S.⁵, Zhou M.⁶, Berline L.¹ and Carlotti F.¹

6
7
8
9
10 ¹Aix Marseille Université, CNRS/INSU, IRD, Mediterranean Institute of Oceanography (MIO),
11 UM 110, Marseille, France

12
13 ²Faculty of Biosciences and Aquaculture, Nord University, N-8049 Bodø, Norway

14
15 ³Department of Earth, Ocean, and Atmospheric Sciences, University of British Columbia, 2207
16 Main Mall, Vancouver, British Columbia, Canada V6T 1Z4

17 ⁴Faculty of Biosciences, Fisheries and Economics, UiT The Arctic University of Norway, N-9037
18 Tromsø

19
20 ⁵Aquatic Ecology Group, Ludwig Maximilian University of Munich (LMU), Grosshadernerstr. 2,
21 82152 Planegg-Martinsried

22
23 ⁶Shanghai Jiao Tong University, Institute of Oceanology, 800 Dongchuan Rd, Minhang, Shanghai,
24 China, 200240

25
26
27
28
29
30
31
32

^{*}Corresponding author: bespinasse@eoas.ubc.ca

33 **Abstract**

34 Recent technical advances in laser-based systems to measure zooplankton distribution have opened
35 new perspectives in ecological and behavioral studies by improving significantly the horizontal
36 and vertical sampling resolution, providing information on zooplankton patchiness and on the
37 influence of small scale physical processes. The application of laser-based systems also led to new
38 challenges on the identification of organisms vs. particulate matter. In areas with high detritus
39 abundances zooplankton abundances might be overestimated by counting plankton and detritus
40 together. We investigated the contribution of detritus in Laser Optical Plankton Counter (LOPC)
41 data collected during two cruises on the continental shelf of the Gulf of Lion (NW Mediterranean
42 Sea). The study area is characterized by several types of ecoregions owing to the influence of
43 winds, freshwater run off and intrusion of oligotrophic waters from offshore. We identified the
44 main mechanisms leading to the formation of detritus as a function of environmental conditions
45 and developed a method to assess the contribution of detritus in LOPC counts based on the
46 proportion of large particles (multi-element plankton, MEPs). Highest percentages of detritus were
47 found in stratified conditions associated with high chl-a concentration (up to 90 % of the counts).
48 Discontinuities in density profiles alone also resulted in peaks of particles concentrations. We
49 suggest a threshold of 2 % of MEPs in LOPC counts above which the LOPC is most likely counting
50 more detritus than organisms. This easy check of the detritus contribution to total LOPC counts
51 was applied to datasets from different marine ecological situations (glacial input, clear water,
52 productive shelf) and proved valid in different biogeographical regions (e.g. high latitude and
53 tropical habitats).

54
55
56
57

58 **Key words:** laser-based sensors, ZooScan, stratification, thin layers, aggregates

59 **1. Introduction**

60 Owing to the high variability of physical processes at small scales and their impacts on biological
61 processes, it is necessary to sample plankton at high resolutions for resolving community structure
62 and dynamics. Based on optical technologies, several optical sensors have been developed in the
63 recent years for high resolution sampling (Benfield et al. 2007). The in-situ sensors are generally
64 based on imaging technologies with relatively low image resolution (e.g. Video Plankton Recorder,
65 Underwater Video Profiler) or based on the transmission or scattering of a laser beam (e.g. Laser
66 Optical Plankton Counter, Laser In-Situ Scattering and Transmissometry). These optical systems
67 not only provide fine resolution vertical profiles but also can sense fragile particles that are
68 generally destroyed when sampling with a net (González-Quirós and Checkley, 2006). Laboratory
69 sensors are mainly based on the high resolution imaging of samples collected with a net or bottles
70 (e.g. FlowCam, ZooScan). Image-based systems allow for the taxonomic identification of
71 organisms up to a certain degree, while the laser-based systems mainly provide sizes and
72 abundances of the organisms studied. The newly developed holographic technology is an
73 exception, but is more similar to in-situ microscopes facing challenges of sampling volume and
74 data processing (Davies et al. 2011, Talapatra et al. 2013). Laser-based systems allow to measure
75 particles in a wide range of sizes and at high frequency but there is a lack of information to
76 distinguish between organisms and particulate matter. The contribution of detritus to presumed
77 zooplankton counts can be problematic in highly productive regions such as fronts, estuarine
78 systems or upwelling areas, where the proportion of detritus in the total particle pool is high so that
79 the size structure of the plankton community cannot be estimated by abundances derived from in-
80 situ laser-based sensors (Zhang et al. 2000, Ohman et al. 2012, Schultes et al. 2013, Basedow et al.
81 2014, Trudnowska et al. 2014).

82 The Laser Optical Plankton Counter (LOPC, Rolls-Royce, England) measures particles and
83 mesozooplankton organisms of sizes between 100 μm and about 3 cm equivalent spherical diameter
84 (ESD) (Herman et al. 2004). It can continuously profile along transects when it is mounted on a
85 Moving Vessel Profiler (MVP, Rolls-Royce, England) (Ohman et al. 2012) or on a glider
86 (Checkley et al. 2008), or can sample vertical profiles when fixed on a net frame or a rosette cage.
87 When particles pass through the tunnel and cross the laser beam, the attenuation of the light
88 intensity is measured by one or several of the 35 photodiode elements, each with 1 mm width. The
89 digital size of a particle is inferred from the intensity changes in shadowed elements, which is
90 converted to ESD. If a particle is recorded by at least 3 diode elements, it will be considered as a
91 multi-element plankton (MEP), in contrast to single element plankton (SEP). In addition to the
92 ESD, more information about the MEPs is provided by the LOPC, allowing to compute an
93 attenuation index (AI). This index has been successfully used to separate detritus and living
94 organisms when targeting large-sized copepods (> 1.5 mm ESD) based on their opacity (Checkley
95 et al. 2008, Gaardsted et al. 2010). For the SEPs, which constitute the dominant part of LOPC
96 counts in the smaller size ranges, no additional information on the transparency of particles is
97 provided, making a direct separation of organisms and detritus impossible. Lately, methods to
98 separate organisms and detritus were proposed, either based on the lognormal distribution expected
99 for size spectra of non-living particles (Petrik et al. 2013, Marcolin et al. 2015) or based on an
100 independent estimation of the size distribution of living organisms from synchronous zooplankton
101 net tows samples (Vandromme et al. 2014).

102 The proportion of detritus to total LOPC counts varies regionally and seasonally (Schultes and
103 Lopes 2009, Gaardsted et al. 2010, Ohman et al. 2012, Petrik et al. 2013, Trudnowska et al. 2014),
104 but the environmental factors influencing this have not been studied in different regions making a
105 general application of thresholds difficult. Here, we use data from winter and spring and from

106 different ecoregions in the Gulf of Lion that are characterized by specific environmental conditions
107 depending on bathymetry, hydrodynamics, atmospheric conditions and freshwater discharge
108 volumes (Espinasse et al. 2014, hereafter E2014; Mermex Group, 2011), to study how
109 environmental conditions influence the LOPC derived indicators AI and %MEPs, and how these
110 reflect the proportion of detritus in LOPC derived abundance. We then apply the thresholds
111 obtained from the Gulf of Lion to a broad range of ecological regions (e.g. polar areas, fjords, open
112 ocean, continental shelf). Our objective is (1) to define the contribution of detritus to particles
113 counted by in-situ laser-based sensors based on environmental parameters and on LOPC derived
114 indicators and (2) to develop thresholds for these indicators to assess the viability of LOPC as
115 zooplankton counter.

116

117 **2. Materials and Methods**

118 The study site is the Gulf of Lion, in the northwestern Mediterranean Sea, which has a large
119 continental shelf up to 80 km wide and a mean depth about 100 m. The hydroclimatic conditions
120 in the gulf are characterized by strong northerly winds, high freshwater input mainly from the
121 Rhône River with an annual mean of $1721 \text{ m}^3 \text{ s}^{-1}$ (Ludwig et al. 2009) and the Northern Current
122 (also called Liguro-Provencal Current) running along the continental slope. This results in several
123 types of ecoregions characterized by specific environmental conditions (E2014).

124 Two research cruises were conducted on board the RV Téthys II, one in spring from 25 April to 2
125 May 2010 (COSTEAU 4) and one in winter from 23 to 27 January 2011 (COSTEAU 6). Each
126 cruise consisted of the same six transects from coast to offshore on the shelf with a total of 135
127 stations sampled with a CTD Rosette system equipped with a LOPC. At 78 out of these 135
128 stations, vertical net tows were conducted within 10 to 30 mn of the CTD-LOPC casts using a 60-
129 cm diameter Bongo frame equipped with two $120 \mu\text{m}$ mesh nets. Net samples were used as the

130 reference for zooplankton abundances allowing to estimate the proportion of detritus in LOPC
131 derived abundance. The LOPC has a flow-through tunnel with an opening of 7×7 cm and was
132 integrated with a data logger and a micro-CTD (Applied Microsystems Ltd, Canada). The sampling
133 rate of LOPC was 2 Hz resulting in a vertical resolution of 0.5 m at 1 m s^{-1} lowering speed.

134

135 2.1. *Environmental conditions*

136 Based on the same cruises, three habitats were defined, characterized by physical parameters such
137 as sea surface salinity, sea surface temperature, bottom potential density, mixed layer depth and
138 stratification index, and biological conditions such as chl-a concentration, particle abundances for
139 3 size classes and the slope of the normalized biomass size spectrum (NBSS) (E2014). Habitat #1
140 was in the near shore area with shallow waters, steep NBSS slope and high chl-a concentration;
141 habitat #2 was representative of the zone of dilution of the Rhône plume with stratified waters and
142 flat NBSS slope; and habitat #3 was on the continental shelf with deep mixed layer depth, lowest
143 particle concentrations and intermediate NBSS slope.

144

145 2.2. *LOPC data processing*

146 Counts and sizes of particles sampled were extracted from the LOPC downcast profiles between 2
147 m depth below the sea surface and 5 m above the sea bottom. Abundance estimates by the LOPC
148 are dependent on the correct estimation of sampled volume (hereinafter SV). SV can either be
149 estimated from flow speed calculated using the manufacturers equation or estimated based on the
150 depth increment acquired together with LOPC counts. Using the manufacturers equation requires
151 that enough particles flow through the sampling tunnel. We used the manufactures equation when
152 the number of particles between 150 and 300 μm was > 30 , otherwise SV was estimated as the
153 product of the LOPC opening area by the depth increment. To avoid duplicate counts of particles

154 that can happen in strong wave conditions, LOPC data for which the depth increment was less than
155 10 cm were removed (5.1 % of the data). All data were processed using an in-house program
156 developed using matlab software (Mathworks, USA). At very high particle densities ($>10^6 \# \text{ m}^{-3}$),
157 the data acquisition frequency of the LOPC might not be sufficient. This results first in incoherent
158 M sequences (data stream containing MEP characteristics), and second in the creation of false
159 MEPs due to the coincidence effect of counting at the same time several neighboring particles as
160 one large particle (Schultes and Lopes 2009, Ohman et al. 2012, Basedow et al. 2014). Incoherent
161 M sequences were observed at 9 out of 135 stations, all of which showed a strong density gradient.
162 If the ratio of MEPs to total LOPC counts (TC) is above 5 % this might indicate coincidence counts
163 (Schultes and Lopes 2009). We observed ratios above 5 % at 5 out of 135 stations, all located near
164 shore.

165

166 2.3. *Net sample processing using ZooScan*

167 An aliquot from each net tow sample was processed using the ZooScan (www.zooscan.com) to
168 calculate the vertically integrated abundances and size structure of the zooplankton communities.
169 Each scanned image had a resolution of 2400 dots per inch and was analyzed using ZooProcess
170 (Gorsky et al. 2010), which is embedded in ImageJ, an image analysis software (Rasband, 2005).
171 A total of 46 variables, including geometrical and optical characteristics, are measured by
172 Zooprocess for each individual larger than 300 μm ESD, and are used by the Plankton Identifier
173 software (Gasparini 2007) to automatically classify the organisms following the supervised
174 learning algorithms implemented in the TANAGRA free statistical pack (Rakotomalala 2005). The
175 Random forest algorithm was used for the classification analysis (Breiman 2001). Two predefined
176 groups were created for the purpose of this study: organisms and detritus. The ‘organisms’ group
177 was mainly constituted of copepods (Carlotti, Unpublished data); and the ‘detritus’ group was a

178 composite category composed of detrital particles, phytoplankton aggregates and undetermined
179 fragments of organisms, such as gelatinous parts, molts etc. Most of these detrital particles are
180 created during the net tow by the pressure of the water against the mesh net and by the aggregation
181 of the material inside the cod-end. Therefore, this detritus cannot be related to those counted in situ
182 by the LOPC and was discarded from the ZooScan counts. After the automatic sorting, all images
183 were validated manually.

184

185 2.4. *Calculation of normalized biomass size spectra*

186 Normalized biomass size spectra (NBSS) were computed from LOPC and ZooScan data. For the
187 ZooScan, the ESD was calculated from the image area of a particle provided by ZooProcess.
188 For both data, the biovolume was derived from the ESD using the formula:

$$189 \quad BioV = ESD^3 \times \frac{\pi}{6 \times \sqrt{R}} \quad (1)$$

190 R , taken equal to 3, is the ratio of the major axis to minor axis of a prolate spheroid and we used
191 an organism density of 1 mg WW mm⁻³ to convert the biovolume into biomass. The NBSS were
192 calculated for each station using the method described in Herman and Harvey (2006). The linear
193 regressions were fitted to the part of a spectrum in the size range starting from the mode of the
194 spectrum in the small size and ending at the first empty size class.

195

196 2.5. *LOPC derived indicators*

197 We investigated two potential indicators that might reflect the proportion of detritus in LOPC
198 counts: (1) the proportion of MEPs in the total number of counts (%MEPs) and (2) the AI indicating
199 the transparency of particles. The theoretical size threshold between SEP and MEP is about 1.5
200 mm (Herman et al. 2004) but MEPs are generally much smaller meaning that they are bigger in

201 size than 1 mm but do not attenuate much light. We hypothesize that, in region where most of the
202 organisms are below 1.5 mm of ESD (about 2.5 mm length for a copepod), the MEPs are mainly
203 composed of detritus so that the %MEPs mainly varies as a function of detritus concentration.
204 The attenuation index (AI) was calculated based on Checkley et al. (2008) and updated by Basedow
205 et al. (2013),

$$206 \quad AI = \sum_{i=2}^{n-1} DS_i \frac{1}{i((n-1)-1) \times \max DS} \quad (2)$$

207 where DS is the digital size of the MEP for each photodiode element, n the number of elements
208 and maxDS is the maximum digital size of a MEP (corresponding to a complete occlusion of a
209 diode element). Based on the definition, AI varies from 0 for very transparent particles to 1 for
210 very opaque particles. The DS values of the elements at the edges of the MEP sequence were not
211 included to compute the AI, because these elements may only partly cover the area of a diode,
212 resulting in a lower AI than real (Basedow et al. 2013). The AI should not be understood as an
213 opacity index only, because both opacity and shape of a particle contribute to it. For example, a
214 filamentous diatom (opaque but with lots of empty space) and an appendicularian (a very
215 transparent organism) could have a similar ESD and AI because they would attenuate the same
216 quantity of light, but they could have very different biovolume and opacity characteristics.

217

218 2.6. Estimation of the detritus part in LOPC counts

219 In the ocean, particulate matter consists of various types of particles including detrital aggregates,
220 decaying fragments of organisms, fecal pellets and sediments (Alldredge and Silver 1988), which
221 will be called detritus hereafter. A total of 78 quasi-synchronous LOPC casts and net tows was
222 analyzed. Because the reliability and accuracy of abundance assessment with the ZooScan is very
223 high, the estimated abundance in the group ‘organisms’ was used as reference for zooplankton

224 abundance in this study. Nevertheless, it is important to keep in mind that nets are biased estimators
225 of the in-situ abundance of organisms that undersample fragile organisms and are limited to a
226 certain size range. Also, net avoidance by mobile organism and net clogging can bias abundance
227 estimates, but were unlikely to be an issue in our study. The size of copepods in the Mediterranean
228 Sea is generally small and the largest individuals of the dominant taxa *Paracalanus* and
229 *Clausocalanus* are about 1 mm length at the adult stage (Gaudy et al. 2003) limiting their escaping
230 capability. Moderate chl-a concentrations (maximum of 2.75 mg m⁻³) measured during the cruises
231 prevented from net clogging (mesh size 120 µm).

232 The size range of zooplankton captured quantitatively is limited by the mesh size for the net
233 samples and the volume filtered for the LOPC (Vandromme et al 2012). Based on the NBSS, we
234 estimated that the valid overlap in size range with correct estimation of abundance from both the
235 ZooScan and LOPC was from 350 µm to 2000 µm ESD.

236 We hypothesize as Vandromme et al (2014) that within this size range the difference between the
237 ZooScan and LOPC is due to particulate matter counted in addition to zooplankton by the LOPC.
238 For size fraction i=350 to 2000 µm, the percentage of detritus in LOPC abundances was calculated
239 following the equation:

$$240 \quad \% \text{ detritus}_i = (\text{LOPC_ab}_i - \text{ZooScan_ab}_i) / \text{LOPC_ab}_i \quad (3)$$

241 ZooScan abundances were higher than LOPC abundances at 12 stations out of 78, albeit only
242 slightly for 9 of them (< 25%), the stations being distributed randomly over the gulf. These stations
243 were not included in the analysis. The factors potentially leading to this situation and the
244 implications for this study are discussed later.

245

246

247

248 2.7. *Statistical analyses*

249 The Kruskal-Wallis test (one way ANOVA on ranks) was performed to identify potential links
250 between the percentage of detritus and LOPC particle characteristics (AI and %MEPs) on one hand,
251 and between percentage of detritus and the zooplankton habitats representative of different
252 environmental conditions on the other hand. This test was chosen because of the non-normal
253 distribution of the variables. Post-hoc tests were performed to assess the differences between
254 habitats. All statistical tests were performed using the R statistical software (R Development Core
255 Team, 2016), Kruskal-Wallis using `kruskal.test` and and post-hoc tests,
256 `posthoc.kruskal.nemenyi.test` (package PCMCRA).

257

258

259

260

261

262

263

264

265

266

267

268

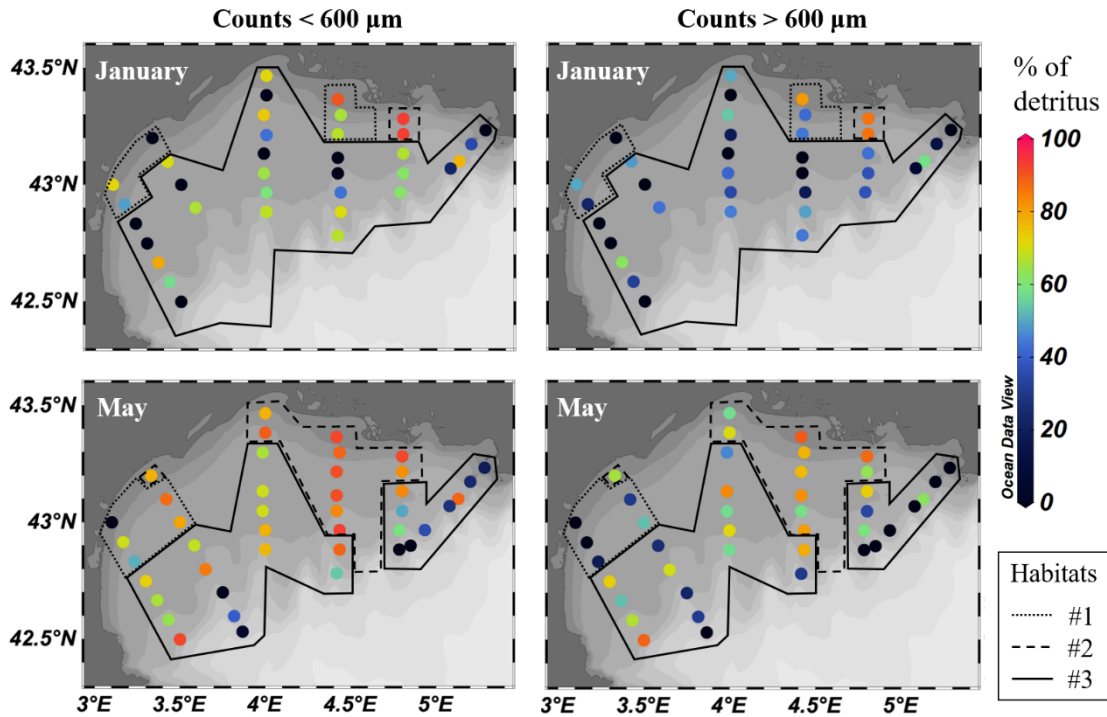
269

270

271

272 3. Results

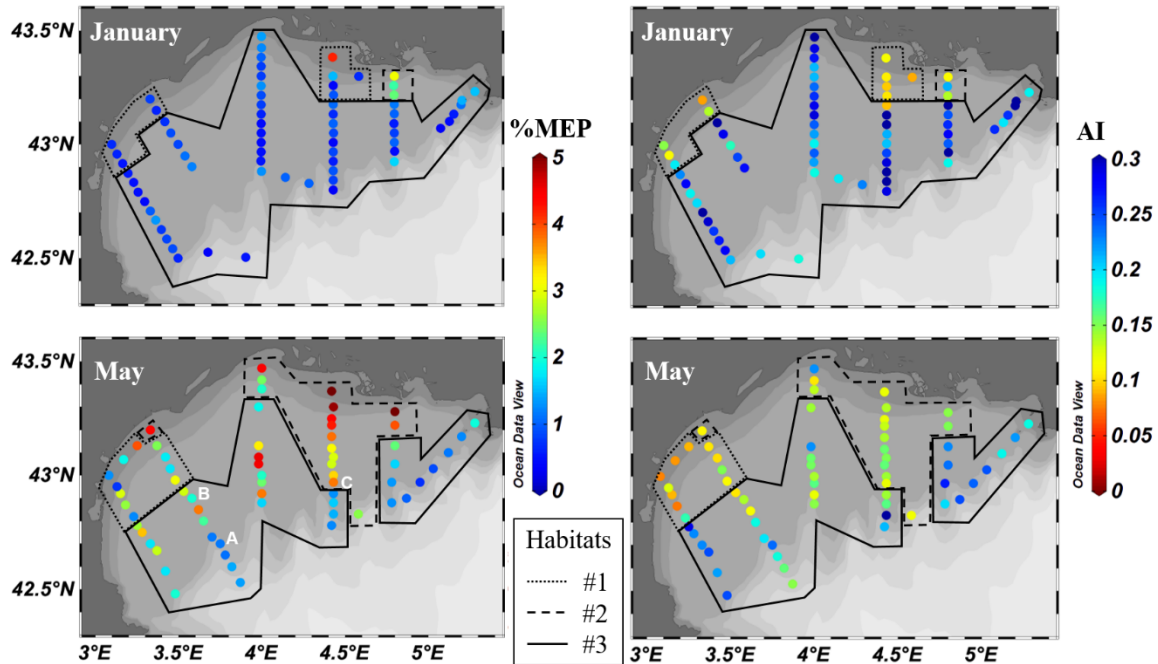
273 3.1. Spatiotemporal distribution of particle characteristics and detritus



274 Fig. 1. Percentage of detritus in LOPC counts in January 2011 (top) and May 2010 (bottom) in the
275 Gulf of Lion for two particle size fractions: below (left) and above (right) 600 μm size. The three
276 habitats defined in Espinasse et al. 2014 are delineated, habitat #1: near shore area; habitat #2: area
277 affected by the Rhône waters; habitat #3: continental shelf.

278
279 The variability of the detritus in terms of spatial and temporal distribution was analyzed for two
280 size fractions, above and below 600 μm ESD (corresponding roughly to a total length of 1 mm for
281 a copepod) (Fig. 1). For both seasons, the percentage of detritus in LOPC counts was lower for the
282 larger size fraction than for the smaller one while their spatial patterns were similar. In winter, the
283 percentage of detritus of both small and large size was relatively low (mainly under 50%), except
284 for the three stations closest to the Rhône mouth. In spring, detritus represented a large part of the

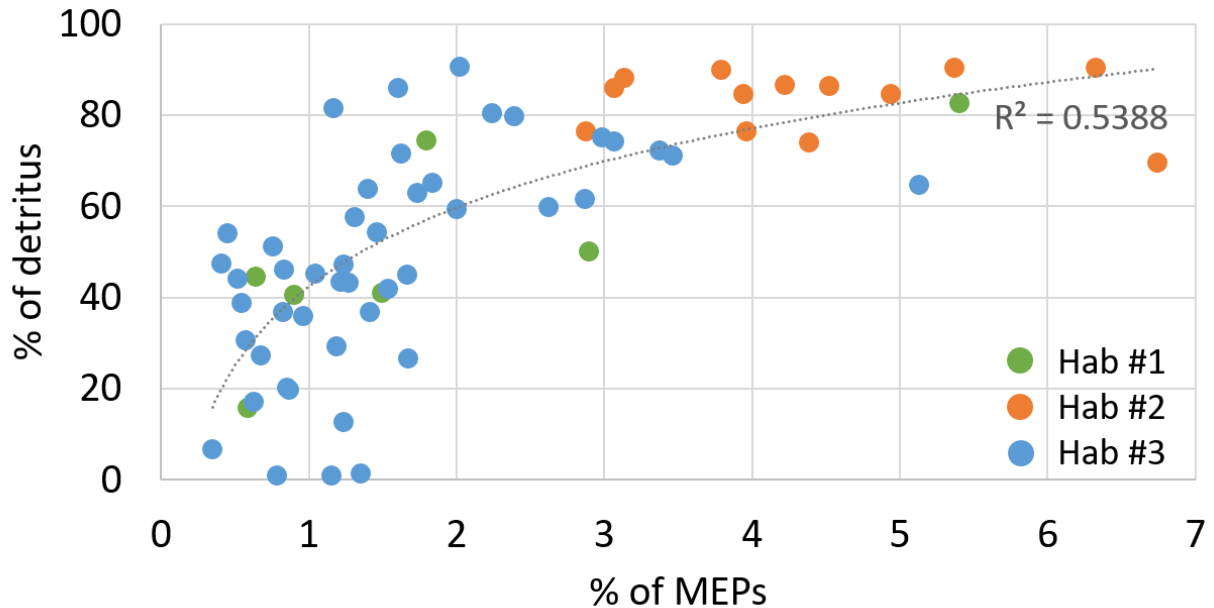
285 LOPC counts (mainly over 50%) in the entire continental shelf. Only at the easternmost transect,
286 influenced by offshore water, a lower percentage of detritus was observed.



287 Fig. 2. Indicators of particles counted by the LOPC in January 2011 (top) and May 2010 (bottom)
288 in the Gulf of Lion: % of MEPs in total LOPC counts (left side) and the MEPs' mean attenuance
289 index (AI, right side). The three habitats defined in Espinasse et al. 2014 are delineated, habitat #1:
290 near shore area; habitat #2: area affected by the Rhône waters; habitat #3: continental shelf. The
291 three representative stations (A, B and C) shown in Fig. 4 are marked in the lower left panel.
292

293 Throughout the study area, spatiotemporal differences in LOPC particle counts and characteristics
294 were observed (Fig. 2). In spring, higher values ($> 2\%$) of the percentage of MEPs in total LOPC
295 counts were generally observed compared to winter ($< 1\%$). However, high values were observed
296 in front of the Rhône mouth in winter and low values beyond the continental slope in spring. The
297 AI of the MEPs showed a pattern rather similar to the %MEPs (Fig.2, right panels). Some
298 differences existed, such as low values for the near shore area in the western part of the gulf in
299 winter and high values for some stations in the most western transect in spring. A highly significant

300 correlation was found between the percentage of detritus and the %MEPs ($r^2=0.54$, $p < 10^{-9}$)
301 strongly supporting our hypothesis that the %MEPs can be used as an indicator of detritus (Fig. 3).
302



303
304 Fig. 3. Percentage of detritus in LOPC counts relative to the percentage of MEPs in total LOPC
305 counts. The data were fitted with a logarithmic function. Habitats as defined in Fig. 1 and 2.

306
307 *3.2. Statistical relationships between environmental conditions and LOPC indicators*
308 To get a better understanding of the mechanisms underlying the relationship between the %MEPs
309 and the detritus abundances, we tracked how they changed with different environmental conditions
310 as described by the three habitats defined in E2014. The percentage of detritus, percentage of MEPs
311 and AI changed significantly between the habitats defined in E2014 (Table 1). The area affected
312 by the Rhône River freshwater (defined as habitat #2) had a significantly higher percentage of
313 detritus and a higher %MEPs than the other two habitats. The average %MEPs in habitat #2 was
314 2.48 (2.18-3.07, $n = 3$) in January and 3.51 (2.07-5.88, $n = 17$) in May compared to an overall

315 average of 1.65 (0.67-4.59, $n = 48$) and 0.67 (0.32-4.18, $n = 67$) for habitats #1 and #3. The
 316 continental shelf (habitat #3) was characterized by particles with a significantly higher AI, overall
 317 average of 0.23 (0.09-0.43, $n = 97$), than for habitats #1 and #2, overall average of 0.11 (0.07-0.19,
 318 $n = 18$) and 0.14 (0.10 – 0.22, $n = 20$), respectively. The changes in distribution of detritus, %MEPs
 319 and AI within the habitats showed that the conditions where stratified waters were coupled with
 320 high chl-a concentrations in the surface layer resulted in a higher percentage of detritus and a higher
 321 %MEPs. This was observed in habitat #2 influenced by Rhône waters. The lower AI and higher
 322 percentage of detritus in habitat #2 demonstrated the general transparency of the detritus, compared
 323 to the higher AI associated with lower detritus observed on the continental shelf (habitat #3).

324

325 Table 1. Kruskal-Wallis test applied on the percentage of detritus, % of MEPs and AI considering
 326 as factors the 3 habitats defined in Espinasse et al. 2014. Post-hoc results are also shown.

327

328

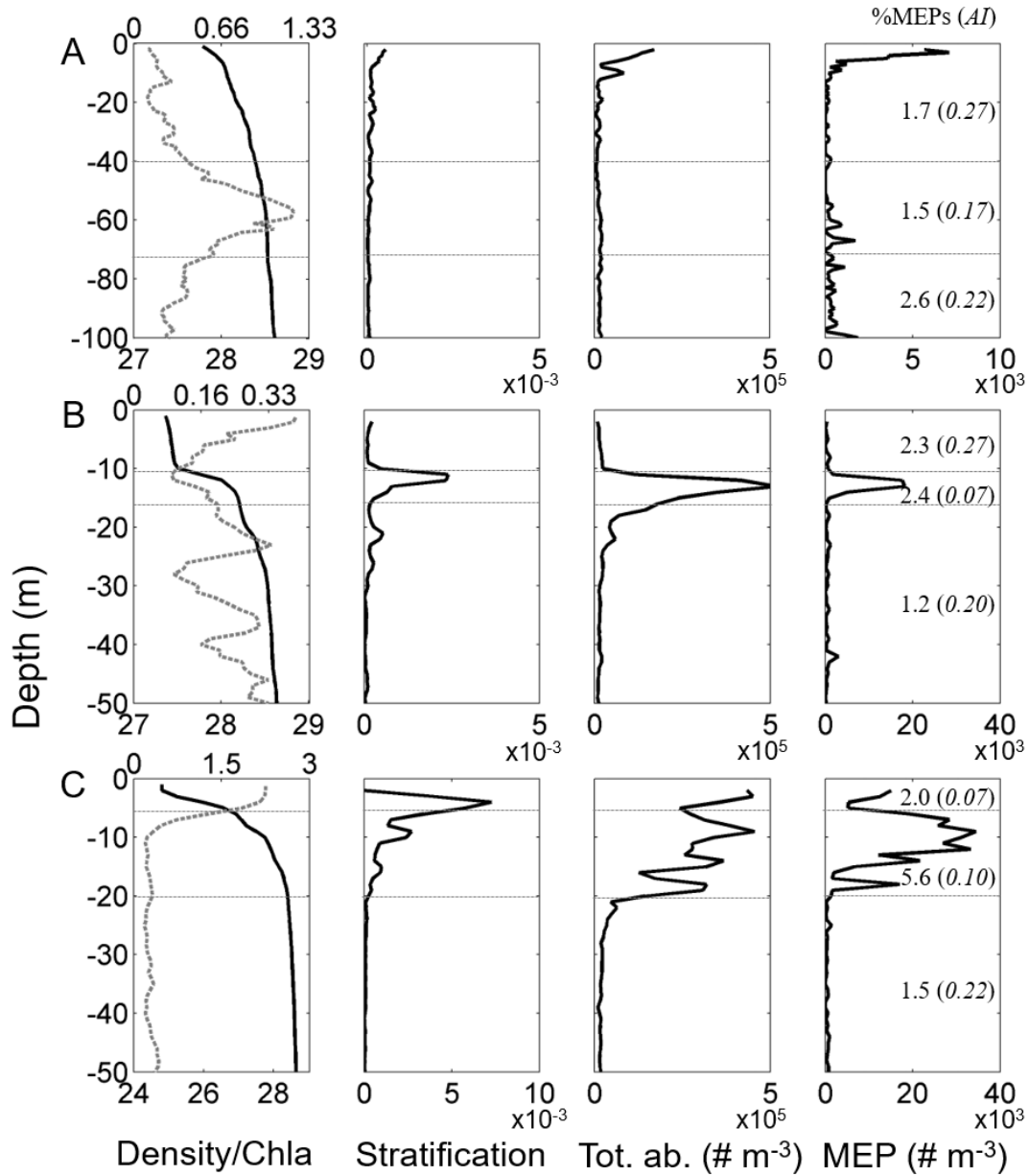
Parameter	X ²	p-value	Post-hoc			
%detritus	25.88	2.39 10 ⁻⁶	Habitat #1	Habitat #2	H2 > H1;	
			Habitat #2	<0.001	-	H2 > H3
			Habitat #3	n.s.	<0.001	
%MEPs	39.09	3.23 10 ⁻⁹	Habitat #1	Habitat #2	H2 > H1;	
			Habitat #2	<0.001	-	H2 > H3
			Habitat #3	n.s.	<0.001	
AI	61.85	3.7 10 ⁻¹⁴	Habitat #1	Habitat #2	H3 > H1;	
			Habitat #2	n.s.	-	H3 > H2
			Habitat #3	<0.001	<0.001	

329

330

331

332



333

334 Fig. 4. Vertical profiles of water density σ_θ (kg m^{-3} ; full line, left panels) and chl-a concentration
 335 (mg m^{-3} ; dashed grey line, left panels), the stratification (Brunt-Väisälä frequency squared N^2 , s^{-2} ;
 336 center left panels), total LOPC abundance (Tot. ab., centre right panels) and MEP abundance (right
 337 panels) at stations A, B and C typical of different environmental conditions. The integrated % of
 338 MEPs and the average of AI are specified in brackets for two (station A) or three (stations B and
 339 C) depth layers (horizontal dotted grey lines). The location of the stations is shown in Fig. 2. Note
 340 the change in x-axis range among stations.

341

342 3.3. *Detailed analyses of particle characteristics at three typical stations*

343 Based on the results provided by the spatial distributions, three stations representing typical
344 environmental conditions in terms of water stratification and chl-a concentration were chosen to
345 investigate the vertical variations of TC, MEPs, %MEPs and AI (Fig. 4).

346 Vertical profiles at station A showed a homogeneous water density and Brunt-Väisälä frequency,
347 and a deep peak of chl-a concentration reaching 1.2 mg chl-a m⁻³ at 60 m depth. TC and MEP
348 counts had a peak in the surface layer, reached minima between 20 and 40 m, and slightly increased
349 in the layer between 40 and 70 m and the layer below, while AI was lower in the layer of maximum
350 of chl-a. At this station, %MEPs and average AI integrated over the entire water column were 1.15
351 and 0.24, respectively, and the percentage of detritus was estimated to be of 0% (i.e. LOPC
352 abundance = ZooScan abundance).

353 Profiles at station B showed a stratified water column with a pycnocline located at 12 m depth and
354 relatively low chl-a concentration (0.09-0.36 mg chl-a m⁻³). TC and MEP counts peaked in the
355 pycnocline layer. The AI was high in the surface layer (0.27) and dropped strongly in the
356 pycnocline layer to 0.07. %MEPs was relatively high in the surface layer and increased below the
357 pycnocline. At this station, %MEPs and average AI integrated over the entire water column were
358 2.00 and 0.14, respectively, and the percentage of detritus was estimated to be of 59% in LOPC
359 counts.

360 Station C was located in the Rhône plume, approximately at 45 km from the Rhône mouth, showing
361 a thin layer of very low salinity water in surface resulting in strong stratification. Highest chl-a
362 concentrations were found in the surface layer (maximum of 2.3 mg chl-a m⁻³). The halocline layer
363 between surface low salinity water and deep saltier water was spread between 5 and 20 m depth.
364 High LOPC abundance and very high MEP abundance were found in the surface and gradient
365 layers. Very low AI values were observed in the surface layer, and low AI values and very high

366 values of %MEPs were found in the halocline. Below the stratified layer these parameters were
367 similar to those at stations A and B. At station C, %MEPs and average AI integrated over the entire
368 water column were 3.79 and 0.12, respectively, and the percentage of detritus was estimated to be
369 up to 90% in LOPC abundance (i.e. LOPC abundance was 10 times the zooplankton abundance
370 estimated with the ZooScan).

371 The NBSSs of particles estimated for the whole water column by both devices showed good
372 agreement in their size range overlap (1.1 to 3.4 log(μg)) for the stations A and B (Fig. 5), but
373 relatively high difference for the station C with higher biomasses from LOPC. NBSS inside the
374 different water layers provides information on the homogeneity of the biomass distribution as a
375 function of depth. The NBSSs at station A were vertically homogeneous, although the biomass in
376 the surface layer was slightly higher. The NBSSs at station B and C showed much higher values in
377 the stratified layers. At station C, the NBSS in the surface layer was characterized by high biomass
378 values in the lower size classes and a steep NBSS slope towards higher size classes, which is a
379 signature of productive layer. In the halocline and below, the NBSS slopes were flatter and similar
380 in shape, potentially resulting from a uniform distribution of the detritus along the size spectrum.

381

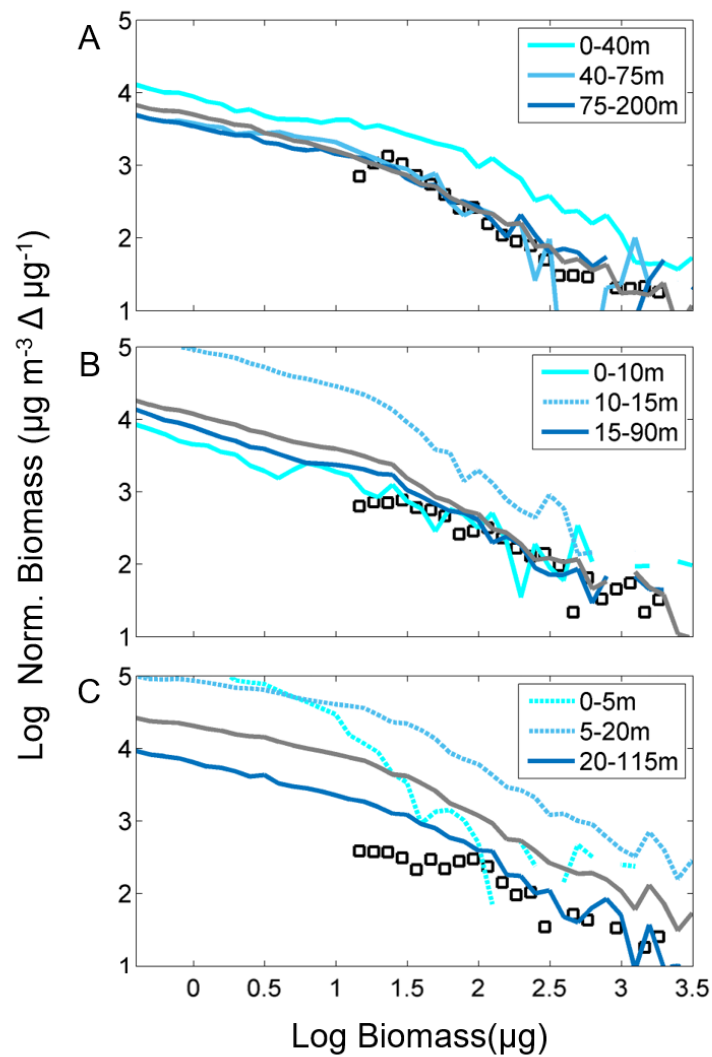
382

383

384

385

386



387 Fig. 5. Normalized biomass size spectra (NBSS) from LOPC data integrated over the water column
 388 (grey line) and in different layers as defined in Fig. 4 (blue lines, NBSSs in stratified layers are
 389 displayed with dashed line), and NBSS from ZooScan data over the whole water column (black
 390 squares) for 3 stations typical of different environmental conditions (see Fig. 2 and 4).

391

392

393

394

395

396 3.4. *Typical distribution of particles and LOPC indicators under specific environmental*
397 *conditions*

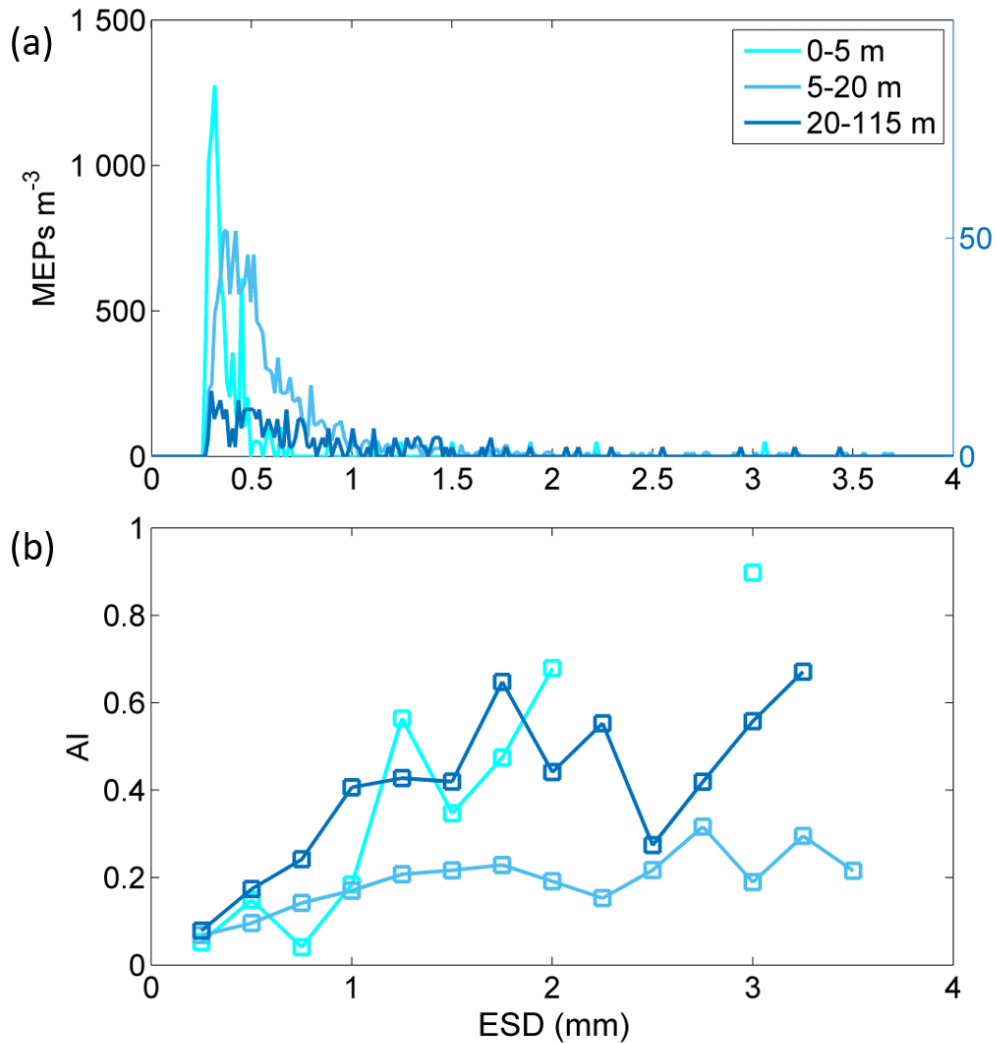
398 Four typical associations between particle distribution and environment could be identified from
399 the detailed analyses of the stations:

400 (1) Vertical density stratification coincided with a peak in LOPC counts. To test this statement, we
401 investigated the occurrences of a peak of LOPC abundance in relation to the occurrences of a
402 strongly stratified layer at all stations. A peak of LOPC counts was defined for concentrations > 50
403 % of the average concentration over the whole profile. Stratified layers were defined using a
404 threshold value of $N^2 = 0.001 \text{ s}^{-2}$ (Brunt-Väisälä frequency). A co-occurrence between a
405 stratification layer and a peak of LOPC counts was found for 93 % of the stations (81 out of 87
406 stations, χ^2 test, $p < 10^{-9}$).

407 (2) The percentage of MEPs in total LOPC counts increased when stratification was associated
408 with high chl-a concentrations ($\text{chl-a} > 1 \text{ mg m}^{-3}$) in the surface layer. Density gradients in the
409 water column typically lead to aggregate formation, and the number of aggregates increase with
410 high production in the surface layer resulting in more MEPs, which is illustrated in the MEP profile
411 and NBSS comparison at station C (Fig. 4 and 5). It was also indirectly confirmed by the changes
412 in AI values as a function of size: larger MEPs ($> 1.5 \text{ mm}$) were very transparent (mean 0.21, std
413 0.10) in the stratified layer compared to the other layers (mean 0.50, std 0.18; Fig. 6b).

414 (3) Situations without stratification and with high chl-a concentrations were associated with a low
415 AI and a relatively low %MEPs (Figs 2 and 4). This situation is exemplified in the surface layer at
416 station C, and to a lesser extent in the middle layer (40 to 75 m depth) at station A. It also
417 corresponds roughly to all the stations within habitat #1, characterized by mixed waters and high
418 chl-a concentrations (Fig. 2). In such situations, the peak in MEP size spectra appears to be shifted
419 towards smaller size classes (Fig. 6a). Accordingly, MEP size in habitat #1 was generally much

420 smaller than in habitat #2 (high chl-a concentration and stratification), with an average of 505 μm
 421 ESD (406-705 μm) and 823 μm ESD (619-1387 μm), respectively.
 422 (4) The AI stayed relatively constant over all the stations without stratification or high chl-a
 423 concentration with an average value of 0.25 (std 0.05).



424 Fig. 6. (a) Size spectra of MEPs and (b) mean attenuation index (AI) as a function of the MEP size
 425 (0.1 mm interval) at station C (see Fig. 2, 4 & 5) in 3 different water layers. Because of lower
 426 values, MEP abundances for the deepest layer (20-115 m) is displayed on a separate axis (right).

427

428

429 **4. Discussion**

430 *4.1. Optimal conditions to use the LOPC as a zooplankton counter*

431 Based on our dataset from the coastal waters of the Northwestern Mediterranean Sea, we identified
432 three main ecological situations where the LOPC counted various amounts of detritus. In
433 unstratified water columns with low chl-a concentrations ($< 1 \text{ mg m}^{-3}$), LOPC abundances were
434 comparable to net abundances, meaning that the LOPC counted mostly zooplankton and only few
435 detritus. This was reflected by LOPC particles having a low %MEPs in total counts ($< 2 \%$), and a
436 high mean AI (> 0.2). In stratified waters with high chl-a concentrations, LOPC abundances were
437 up to ten times higher than net abundances most likely due to the LOPC counting detritus. In this
438 situation, LOPC counts were characterized by high %MEPs and low AIs. In stratified waters with
439 low chl-a concentrations, LOPC abundances were also higher than net abundances but in a lesser
440 extent, and particles here were again characterized by a high %MEPs and a low AI. These results
441 suggest that information on the large particles counted by the LOPC (MEPs) can be used to infer
442 the percentage of detritus counted by the LOPC. Our results also suggest that the LOPC counted
443 mainly living organisms when the %MEPs was $< 2 \%$, a more conservative limit than the 5% limit
444 found by Schultes and Lopes (2009) off the Brazilian coast. In most water columns without
445 stratification and/or high chl-a concentration the mean AI remained constant, around 0.25, which
446 allowed us to define a threshold below which aggregation or phytoplankton chains likely occur.
447 The usage of %MEPs and AI as indicators of different physical and biological situations is
448 summarized in Table 2. By applying our thresholds to the data from our study area and to data from
449 high latitudes, we could identify in total four different situations in which detritus represent
450 between 0 and 90 % of the total LOPC counts.

451

452

453 Table 2. Summary describing how to interpret the LOPC abundance with the help of the two
 454 indicators, %MEPs and AI, and typical situations leading to these indicator values.

	Low AI (< 0.2)	High AI (> 0.2)
High % of MEPs (> 2) (> 5 overestimation)	Aggregate formation if stratified waters, can be promoted by high primary production	High concentration of big copepods (> 1.5 mm), mainly in high latitude areas, or terrestrial input (sand)
Low % of MEPs (< 2)	Low detritus, if high chl-a concentration, phytoplankton chains or colonies characterized by small MEP size (< 400 µm ESD)	Clear water, LOPC mainly counting zooplankton

455

456

457 4.2. *Potential biases linked to the sampling protocol*

458 The LOPC was placed on the CTD rosette to obtain simultaneous profiles of physical and
 459 biogeochemical parameters and net tows were conducted afterwards. The time lag between a LOPC
 460 cast and corresponding net tow could have affected the comparison between ZooScan and LOPC
 461 results, even though it was reduced to its minimum. The general patchiness of particles and
 462 zooplankton in the water column can create some variability in abundance data collected at the
 463 same location over a short amount of time. At 3 out of 78 stations, abundances determined from
 464 net samples were >25 % higher than those determined by the LOPC, possibly due to a patchy
 465 distribution. In general however, the vertical distributions of particles measured by the LOPC along
 466 the coastal-offshore transects (stations separated by 5 km) showed consistent abundances between
 467 the stations with gradual changes, suggesting a limited patchiness. Furthermore, for the majority

468 of the offshore stations with no stratification and low chl-a concentration, the percentage of detritus
469 was intermediate and rather constant (mean 39, standard deviation 17). Therefore, we argue that
470 even if patchiness potentially created some variability blurring our results, at most of our stations
471 it was valid to use a comparison of abundances, determined from net samples and based on LOPC,
472 to determine the detritus contribution.

473

474 4.3. *Impact of stratification and/or high production on LOPC counts and the formation*
475 *of MEPs*

476 The relationship between the detritus distribution and the habitats defined in E2014 (Table 1)
477 provided a good base to analyze the link between detritus formation and environmental conditions.
478 Consistent results were found analyzing the spatial distributions and the vertical profiles in the
479 changes of percentage of detritus, LOPC counts and MEP characteristics. The stratification of the
480 water column seems to be the main factor influencing the vertical distribution of LOPC counts.
481 The interface between water layers of different densities acts as a barrier, locally accumulating
482 particles. The high concentrations of particles within pycnoclines can be explained by the change
483 in buoyancy of aggregates, reducing their downward settling velocities (Macintyre *et al.*, 1995,
484 Prairie *et al.*, 2015). Our case study from the Mediterranean Sea shows that this process induces
485 particle aggregations resulting in the formation of transparent MEPs with a low AI (< 0.2), and in
486 an increase of the %MEPs in total counts (see again Fig. 1, situation described in the upper left part
487 of the Table 2). The mechanisms underlying the aggregate formation can be mechanical, due to
488 transparent exopolymer particles, mucus or dead phytoplankton cells (Alldredge and Silver, 1988),
489 or chemical, when strong salinity changes promotes flocculation processes. When such a
490 stratification is combined with high production in the surface layer, the higher concentration of
491 particles will promote the formation of more aggregates, resulting in very high %MEPs.

492 When high chl-a concentrations were not associated with stratification, the size of the MEPs was
493 smaller and the AI decreased below 0.2 while the %MEPs remained constant. One explanation is
494 that without stratification, settling particles could freely fall through the water column, and the
495 probability of colliding between particles is reduced. But also, phytoplankton colonies typically
496 produce small MEPs with lower AI due to a high degree of empty space at the activated
497 photodiodes.

498

499 4.4. *Limits of the methods*

500 Our method is based on the information from the MEPs, which represent only a small part of the
501 LOPC counts, but we successfully extrapolated this result to assess the contribution of detritus in
502 the total LOPC counts. We suggest that there is a relationship between the % of SEPs being detritus
503 and the %MEPs in LOPC counts. Indeed, the aggregation processes described earlier in the text
504 (see 4.3) attest that if detritus represents a substantial part of the SEPs, some will aggregate and
505 end up as MEPs. This is due to the detritus constitution and has been described by several studies
506 focusing, for instance, on phytoplankton blooms (Alldredge and Jackson, 1995) or appendicularian
507 houses (Lombard and Kiørboe, 2010).

508 In some specific cases the %MEPs can be affected by others causes than the ones described in this
509 study. In places with very clear water and high concentrations of big organisms, e.g. *Calanus*
510 *finmarchicus* overwintering in North Atlantic waters, the %MEPs can drastically rise even though
511 the percentage of detritus is low (Table 2, upper right). In that case, we suggest to use the AI alone
512 as an indicator to separate between living and non-living particles (Checkley et al. 2008, Gaardsted
513 et al. 2010), and estimate the part of the MEPs being detrital particles. In this study, where the
514 dominating species were small copepods, we assume that MEPs that have a low AI were detritus.
515 However, transparent gelatinous organisms can also have similar MEP signal. Given the opening

516 of the LOPC tunnel (7 x 7 cm), appendicularians are among potential organisms that can be counted
517 by the LOPC in amounts high enough to affect the MEP signal. In our case, although substantial
518 abundance of appendicularians were recorded during the winter cruise (ca 30 000 # m⁻²), this did
519 not seem to affect the MEP signal as the AI was higher in winter than during the spring cruise.
520 Nevertheless, we suggest that when using the LOPC, occasional net samples are needed to describe
521 the plankton community and to attest of peaks of specific groups such as gelatinous zooplankton.

522

523 4.5. *Validity of our results in other regions*

524 The indicators developed in this study to interpret the detritus part of LOPC abundances are based
525 on a large dataset collected in a coastal area of the NW Mediterranean Sea. However, the processes
526 leading to the formation of detritus are not specific to this area. They take place in the epipelagic
527 zone of most of the marine ecosystems, and it is likely that these indicators will be valid in other
528 areas. To test this, we applied the thresholds for %MEPs and AI that were developed in this study
529 to other datasets from around the globe.

530 A dataset collected in a tropical system (Schultes and Lopes 2009), sampled from unstratified
531 stations over the continental shelf and slope, had generally a low %MEPs (mean 0.87, standard
532 deviation 0.33) and rather high AIs (mean 0.22, standard deviation 0.04) over 37 stations (Table
533 3). The biomass estimated with the LOPC for particles > 500 µm ESD was significantly correlated
534 to zooplankton displacement volume of net samples, indicating a limited influence of detritus
535 (Table 2, lower right).

536 Two datasets from polar areas (Antarctic Peninsula and Svalbard) were characterized by clear
537 water, and LOPC counts had a very low %MEPs (< 0.5 %) and generally high AIs (> 0.2). Here,
538 the indicators show that the LOPC counted mainly zooplankton (Table 2, lower right).

539 In an Arctic fjord characterized by glacial melt water input, freshwater run-off resulted in a
540 dramatic increase in LOPC counts ($> 500 \times 10^3 \# \text{ m}^{-3}$) in the inner part of the fjord and very low
541 AI values in the entire fjord (Trudnowska *et al.*, 2014). The %MEPs, on the other hand, was
542 gradually decreasing from 3.90 in the inner part to 1.16 in the outer part. Based on the thresholds
543 developed for the indicators %MEPs and AI, the fjord can be divided into two areas, i.e. the inner
544 part characterized by high %MEPs, low AIs and high (glacial) detritus concentrations (Table 2,
545 upper right); and the outer part characterized by low %MEPs, low AIs, high chl-a concentration
546 and realistic zooplankton abundances estimated by the LOPC (Table 2, lower left).

547

548

549

550

551

552

553

554

555

556

557

558

559

560

561

562

563 Table 3. Comparison of particle characteristics in different regions and different environmental
 564 conditions. Only stations deeper than 50 m were included. High chl-a: max chl-a > 1 mg m⁻³.

Environmental conditions	Region / remarks	# part m ⁻³ min-max nbr. of stn.	AI mean (min-max)	%MEPs mean (min-max)	References
Mixed waters	Antarctic Peninsula – Continental bay Clear water and few large-sized organisms	3600 – 36200 <i>n=16</i>	0.24 (0.09 – 0.54)	0.34 (0.16 – 1.61)	Espinasse et al. 2012
	Svalbard – Cross shelf section	2000 – 26000 <i>n=10</i>	0.48 (0.36 – 0.56)	0.33 (0.14 – 2.17)	Basedow Unpublished data
	North Atlantic – Open ocean Very clear water	4000 – 6000 <i>n=3</i>	0.46 (0.31 – 0.62)	0.76 (0.70 – 0.85)	Basedow et al. 2016
	Brazil coast – Continental slope	6900 – 146000 <i>n=37</i>	0.22 (0.13 – 0.3)	0.87 (0.54 – 2.04)	Schultes and Lopes 2009
	NW Mediterranean Sea – Continental slope	18000 – 30000 <i>n=43</i>	0.25 (0.11 – 0.44)	0.90 (0.40 – 1.92)	This study
	Polar fjord – Outer part high chl-a	130000 – 240000 <i>n=2</i>	0.10 (0.08 – 0.11)	1.16 (0.71 – 1.61)	Trudnowska et al. 2014
Stratified waters	Polar fjord – Glacier area Input of particles from melt-water discharge	475000 – 865000 <i>n=4</i>	0.08 (0.07 – 0.08)	3.90 (2.27 – 6.25)	Trudnowska et al. 2014
	NW Mediterranean Sea - Continental shelf	48000 – 70000 <i>n=8</i>	0.15 (0.11 – 0.22)	2.08 (1.13– 4.01)	This study
Stratified waters + high chl-a	NW Mediterranean Sea - Freshwater run-off	100000 – 215000 <i>n=13</i>	0.12 (0.07 – 0.14)	3.21 (1.70 – 5.36)	This study

565

566 **5. Conclusion**

567 We defined thresholds for two indicators based on LOPC data, which allowed to quickly check the
568 contribution of detritus to total LOPC counts. These indicators were developed based on an
569 extensive dataset from the Gulf of Lion and proved valid in different marine biogeographical
570 regions. Applying the indicators %MEPs and AI provides a good basis to assess the detrital part in
571 LOPC counts. When the thresholds for %MEPs and AI indicate that the LOPC is not mainly
572 counting zooplankton, data should be interpreted carefully with respect to environmental data and
573 the zooplankton community. This is especially important in shallow coastal waters, and more
574 generally in strongly stratified waters. Here, LOPC data and other laser-based sensors should
575 always be interpreted in parallel with a complementary dataset providing an independent estimate
576 of the zooplankton part in particle counts.

577

578

579

580

581

582 **Acknowledgments**

583 This study is a contribution to the MERMEX-MISTRALS-WP2 'Ecological Processes'. The
584 research cruises and laboratory analysis were supported by the project ANR COSTAS (ANR-09-
585 CESA-007-04), whereas optical sensors implemented and used during the cruises were funded by
586 ANR FOCEA (ANR-09-CEXC-006-01). The authors are grateful to the crews of the R/V Tethys
587 II and SAM-M I O platform for their operation at sea. The postdoctoral fellowship of BE was
588 funded in the frame of the ConocoPhillips *Calanus* project (NSBU-107021) lead by the research
589 network ARCTOS.

590 **References**

- 591 Alldredge, A., Gotschalk, C.C., 1988. In situ settling behavior of marine snow. *Limnology and*
592 *Oceanography*, 33, 339-351.
- 593 Alldredge, A.L., Jackson, G.A., 1995. Preface: Aggregation in marine system. *Deep Sea Research*
594 *Part II: Topical Studies in Oceanography*, 42, 1-7.
- 595 Basedow, S.L., de Silva, N.A.L., Bode, A., van Beusekorn, J., 2016. Trophic positions of
596 mesozooplankton across the North Atlantic: estimates derived from biovolume spectrum
597 theories and stable isotope analyses. *Journal of Plankton Research*, 38, 1364-1378.
- 598 Basedow, S.L., Tande, K.S., Norrbin, M.F., Kristiansen, S.A., 2013. Capturing quantitative
599 zooplankton information in the sea: Performance test of laser optical plankton counter and video
600 plankton recorder in a *Calanus finmarchicus* dominated summer situation. *Progress in*
601 *Oceanography*, 108, 72-80.
- 602 Basedow, S.L., Zhou, M., Tande, K.S., 2014. Secondary production at the Polar Front, Barents
603 Sea, August 2007. *Journal of Marine Systems*, 130, 147-159.
- 604 Benfield, M.C., Grosjean, P., Culverhouse, P.F., Irigoien, X., Sieracki, M.E., Lopez-Urrutia, A.,
605 Dam, H.G., Hu, Q., Davis, C.S., Hansen, A., Pilskaln, C.H., Riseman, E.M., Schultz, H., Utgoff,
606 P.E., Gorsky, G., 2007. Research on automated plankton identification. *Oceanography*, 20, 172-
607 187.
- 608 Breiman, L., 2001. Random forests. *Mach. Learn.*, 45, 5-32.
- 609 Checkley, D.M., Jr., Davis, R.E., Herman, A.W., Jackson, G.A., Beanlands, B., Regier, L.A., 2008.
610 Assessing plankton and other particles in situ with the SOLOPC. *Limnology and Oceanography*,
611 53, 2123-2136.
- 612 Davies, E.J., Nimmo-Smith, W.A.M., Agrawal, Y.C., Souza, A.J., 2011. Scattering signatures of
613 suspended particles: an integrated system for combining digital holography and laser diffraction.
614 *Opt. Express*, 19, 25488-25499.
- 615 Espinasse, B., Carlotti, F., Zhou, M., Devenon, J., 2014. Defining zooplankton habitats in the Gulf
616 of Lion (NW Mediterranean Sea) using size structure and environmental conditions. *Marine*
617 *Ecology Progress Series*, 506, 31-46.
- 618 Espinasse, B., Zhou, M., Zhu, Y., Hazen, E., Friedlaender, A., Nowacek, D., Chu, D., Carlotti, F.,
619 2012. Austral fall-winter transition of mesozooplankton assemblages and krill aggregations in
620 an embayment west of the Antarctic Peninsula. *Marine Ecology Progress Series*, 452, 63-80.
- 621 Gaardsted, F., Tande, K.S., Basedow, S.L., 2010. Measuring copepod abundance in deep-water
622 winter habitats in the NE Norwegian Sea: intercomparison of results from laser optical plankton
623 counter and multinet. *Fisheries Oceanography*, 19, 480-492.
- 624 Gasparini, S., 2007. PLANKTON IDENTIFIER: a software for automatic recognition of
625 planktonic organisms., http://www.obs-vlfr.fr/~gaspari/Plankton_Identifier/index.php.
- 626 Gaudy, R., Youssara, F., Diaz, F., Raimbault, P., 2003. Biomass, metabolism and nutrition of
627 zooplankton in the Gulf of Lions (NW Mediterranean). *Oceanologica Acta*, 26, 357-372.
- 628 González-Quirós, R., Checkley, D.M., Jr., 2006. Occurrence of fragile particles inferred from
629 optical plankton counters used in situ and to analyze net samples collected simultaneously. *J.*
630 *Geophys. Res.*, 111, C05S06.
- 631 Gorsky, G., Ohman, M.D., Picheral, M., Gasparini, S., Stemmann, L., Romagnan, J.-B., Cawood,
632 A., Pesant, S., García-Comas, C., Prejger, F., 2010. Digital zooplankton image analysis using
633 the ZooScan integrated system. *Journal of Plankton Research*, 32, 285-303.
- 634 Herman, A.W., Beanlands, B., Phillips, E.F., 2004. The next generation of Optical Plankton
635 Counter: the Laser-OPC. *Journal of Plankton Research*, 26, 1135-1145.

636 Herman, A.W., Harvey, M., 2006. Application of normalized biomass size spectra to laser optical
637 plankton counter net intercomparisons of zooplankton distributions. *Journal of Geophysical*
638 *Research*, 111, 1-9.

639 Lombard, F., Kiørboe, T., 2010. Marine snow originating from appendicularian houses: Age-
640 dependent settling characteristics. *Deep Sea Research I*, 57, 1304-1313.

641 Ludwig, W., Dumont, E., Meybeck, M., Heussner, S., 2009. River discharges of water and nutrients
642 to the Mediterranean and Black Sea: Major drivers for ecosystem changes during past and future
643 decades? *Progress in Oceanography*, 80, 199-217.

644 MacIntyre, S., Alldredge, A.L., Gotschalk, C.C., 1995. Accumulation of Marine Snow at Density
645 Discontinuities in the Water Column. *Limnology and Oceanography*, 40, 449-468.

646 Marcolin, C.d.R., Schultes, S., Jackson, G.A., Lopes, R.M., 2013. Plankton and seston size spectra
647 estimated by the LOPC and ZooScan in the Abrolhos Bank ecosystem (SE Atlantic).
648 *Continental Shelf Research*, 70, 74-87.

649 Marcolin, C.R., Lopes, R.M., Jackson, G.A., 2015. Estimating zooplankton vertical distribution
650 from combined LOPC and ZooScan observations on the Brazilian Coast. *Marine Biology*, 162,
651 2171-2186.

652 Mermex group, 2011. Marine ecosystems responses to climatic and anthropogenic forcings in the
653 Mediterranean. *Progress in Oceanography*, 91, 97-166.

654 Ohman, M.D., Powell, J.R., Picheral, M., Jensen, D.W., 2012. Mesozooplankton and particulate
655 matter responses to a deep-water frontal system in the southern California Current System.
656 *Journal of Plankton Research*, 34, 815-827.

657 Petrik, C.M., Jackson, G.A., Checkley Jr, D.M., 2013. Aggregates and their distributions
658 determined from LOPC observations made using an autonomous profiling float. *Deep Sea*
659 *Research Part I: Oceanographic Research Papers*, 74, 64-81.

660 Prairie, J.C., Ziervogel, K., Camassa, R., McLaughlin, R.M., White, B.L., Dewald, C., Arnosti, C.,
661 2015. Delayed settling of marine snow: Effects of density gradient and particle properties and
662 implications for carbon cycling. *Marine Chemistry*, 175, 28-38.

663 R Development Core Team, 2017. *R: A language and environment for statistical computing*.
664 Vienne, Austria: R Foundation for Statistical Computing.

665 Rakotomalala, R., 2005. TANAGRA : un logiciel gratuit pour l'enseignement et la recherche. *In :*
666 *Actes de EGC 2005*, 2, 697-702.

667 Rasband, W.S., 2005. ImageJ. US National Institutes of Health, Bethesda, MD.

668 Schultes, S., Lopes, R.M., 2009. Laser Optical Plankton Counter and Zooscan intercomparison in
669 tropical and subtropical marine ecosystems. *Limnology and Oceanography: Methods*, 7, 771-
670 784.

671 Schultes, S., Sourisseau, M., Le Masson, E., Lunven, M., Marié, L., 2013. Influence of physical
672 forcing on mesozooplankton communities at the Ushant tidal front. *Journal of Marine Systems*,
673 109-110, Supplement, S191-S202.

674 Talapatra, S., Hong, J., McFarland, M., Nayak, A., Zhang, C., Katz, J., Sullivan, J., Twardowski,
675 M., Rines, J., Donaghay, P., 2013. Characterization of biophysical interactions in the water
676 column using in situ digital holography. *Marine Ecology Progress Series*, 473, 29-51.

677 Trudnowska, E., Basedow, S.L., Blachowiak-Samolyk, K., 2014. Mid-summer mesozooplankton
678 biomass, its size distribution, and estimated production within a glacial Arctic fjord (Hornsund,
679 Svalbard). *Journal of Marine Systems*, 137, 55-66.

680 Vandromme, P., Nogueira, E., Huret, M., Lopez, U., Aacute, González-Nuevo González, G.,
681 Sourisseau, M., Petitgas, P., 2014. Springtime zooplankton size structure over the continental
682 shelf of the Bay of Biscay. *Ocean Science*, 10, 821-835.

683 Zhang, X., Roman, M., Sanford, A., Adolf, H., Lascara, C., Burgett, R., 2000. Can an optical
684 plankton counter produce reasonable estimates of zooplankton abundance and biovolume in
685 water with high detritus? *Journal of Plankton Research*, 22, 137-150.

686

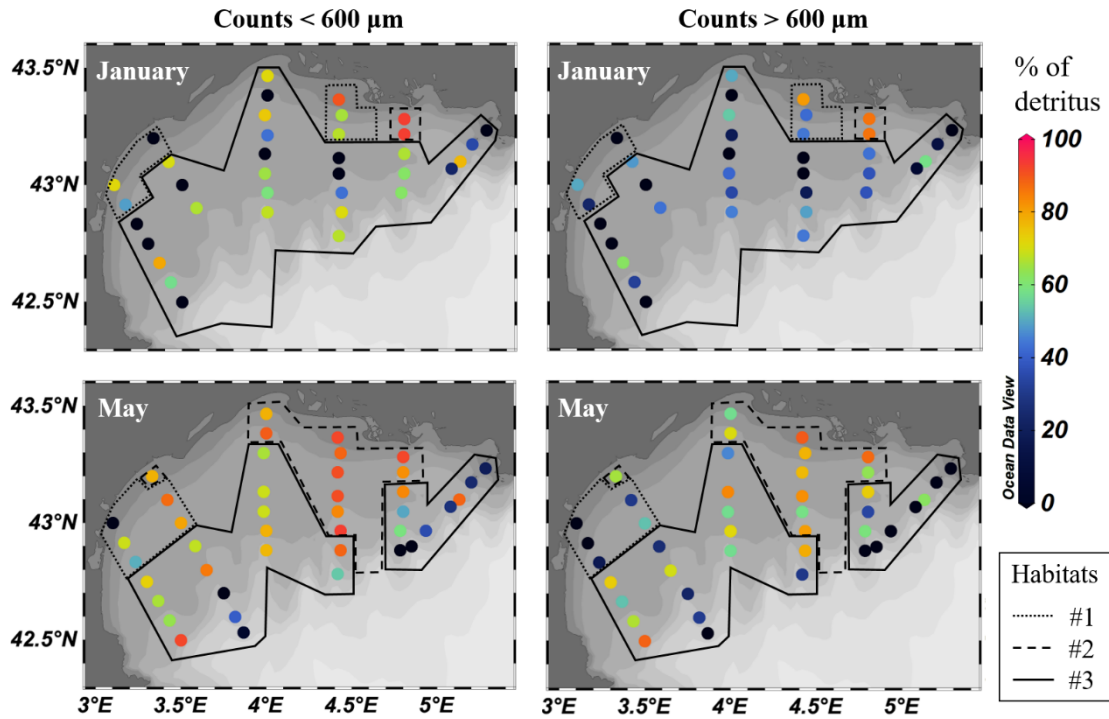


Fig. 1. Percentage of detritus in LOPC counts in January 2011 (top) and May 2010 (bottom) in the Gulf of Lion for two particle size fractions: below (left) and above (right) 600 μm size. The three habitats defined in Espinasse et al. 2014 are delineated, habitat #1: near shore area; habitat #2: area affected by the Rhône waters; habitat #3: continental shelf.

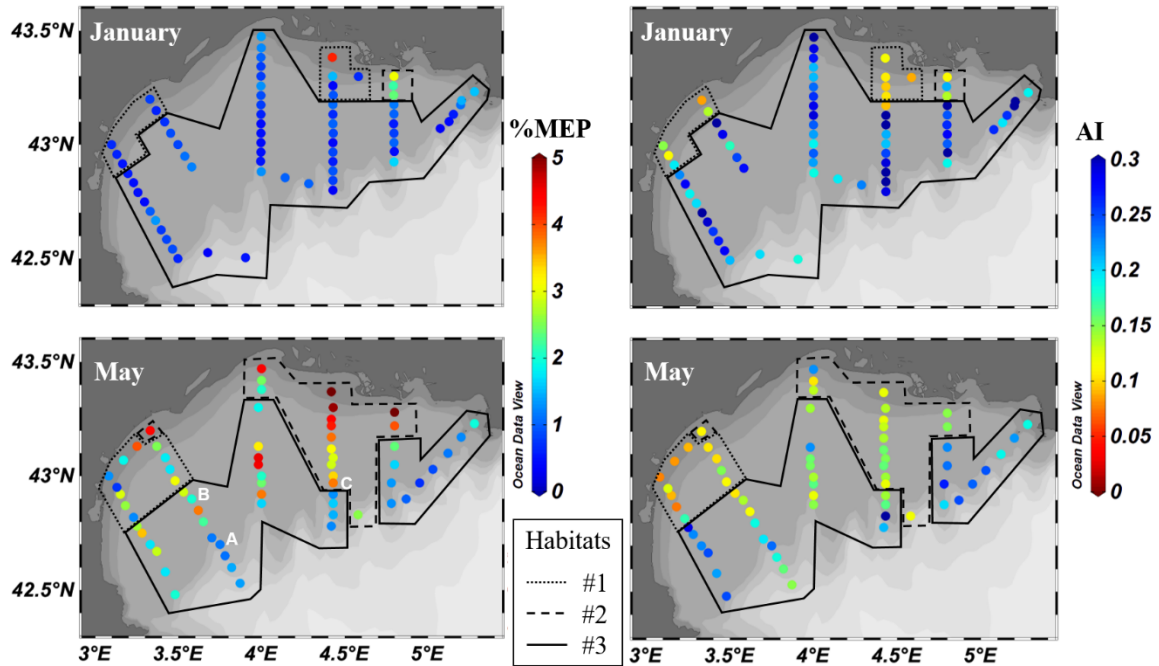


Fig. 2. Indicators of particles counted by the LOPC in January 2011 (top) and May 2010 (bottom) in the Gulf of Lion: % of MEPs in total LOPC counts (left side) and the MEPs' mean attenuation index (AI, right side). The three habitats defined in Espinasse et al. 2014 are delineated, habitat #1: near shore area; habitat #2: area affected by the Rhône waters; habitat #3: continental shelf. The three representative stations (A, B and C) shown in Fig. 4 are marked in the lower left panel.

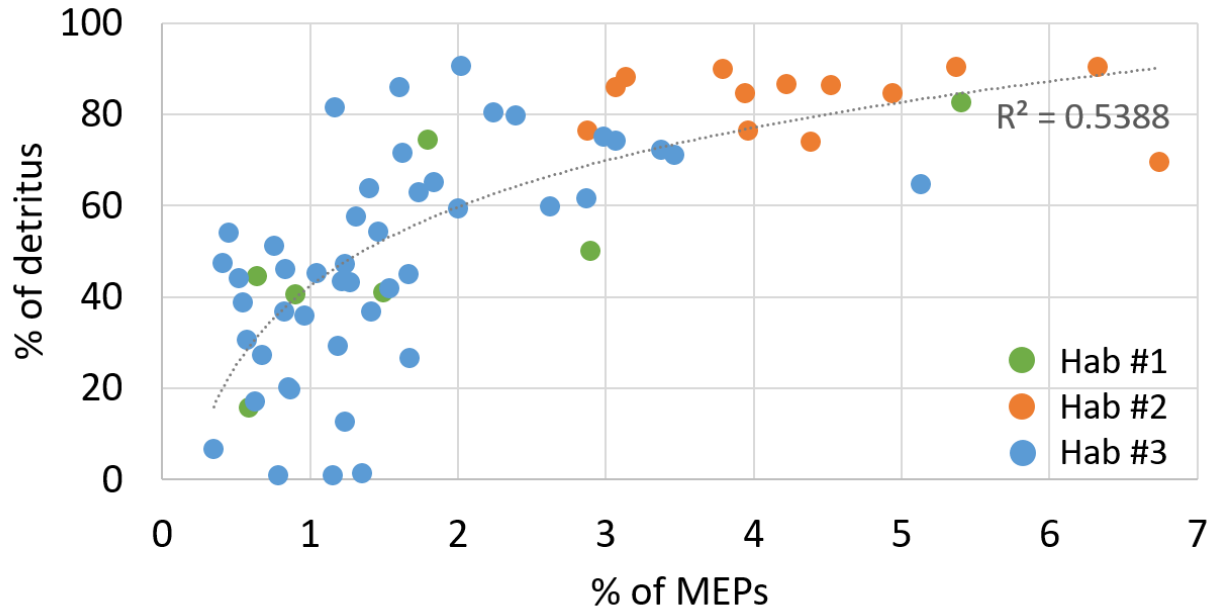


Fig. 3. Percentage of detritus in LOPC counts relative to the percentage of MEPs in total LOPC counts. The data were fitted with a logarithmic function. Habitats as defined in Fig. 1 and 2.

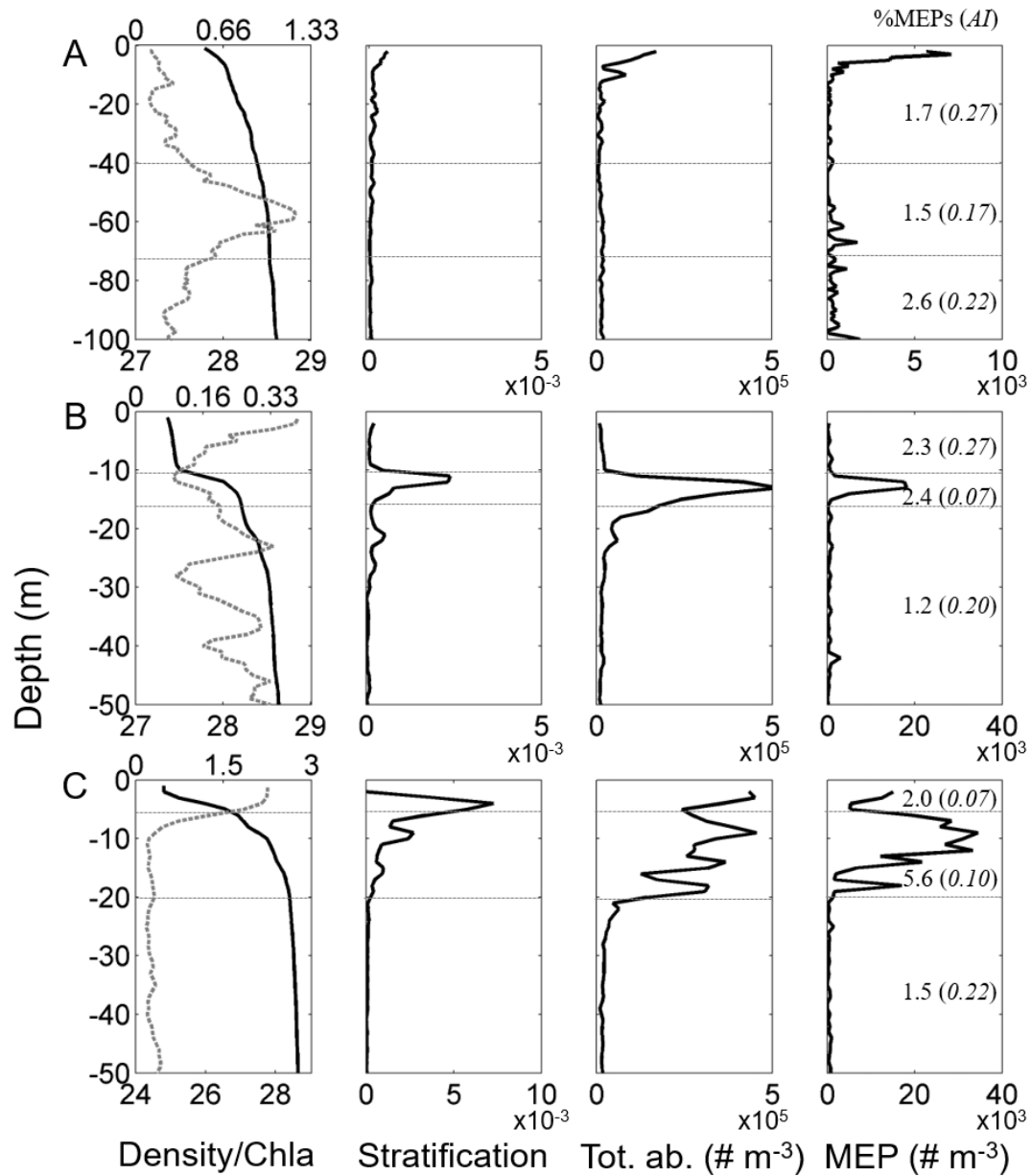


Fig. 4. Vertical profiles of water density σ_θ (kg m^{-3} ; full line, left panels) and chl-a concentration (mg m^{-3} ; dashed grey line, left panels), the stratification (Brunt-Väisälä frequency squared N^2 , s^{-2} ; center left panels), total LOPC abundance (Tot. ab., centre right panels) and MEP abundance (right panels) at stations A, B and C typical of different environmental conditions. The integrated % of MEPs and the average of AI are specified in brackets for two (station A) or three (stations B and C) depth layers (horizontal dotted grey lines). The location of the stations is shown in Fig. 2. Note the change in x-axis range among stations.

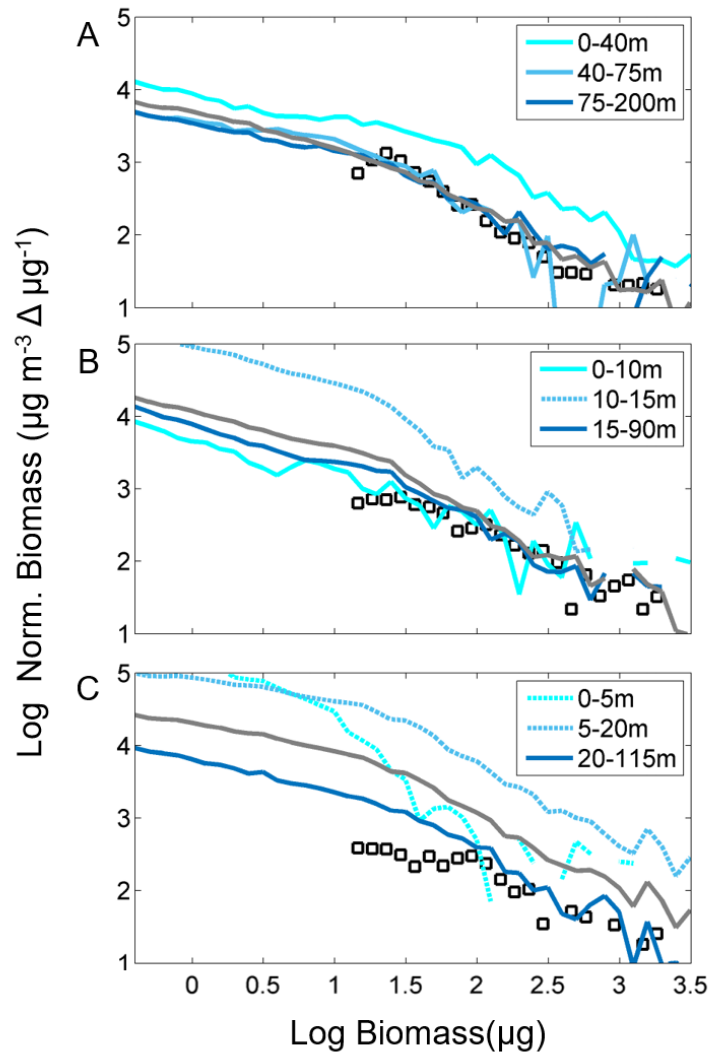


Fig. 5. Normalized biomass size spectra (NBSS) from LOPC data integrated over the water column (grey line) and in different layers as defined in Fig. 4 (blue lines, NBSSs in stratified layers are displayed with dashed line), and NBSS from ZooScan data over the whole water column (black squares) for 3 stations typical of different environmental conditions (see Fig. 2 and 4).

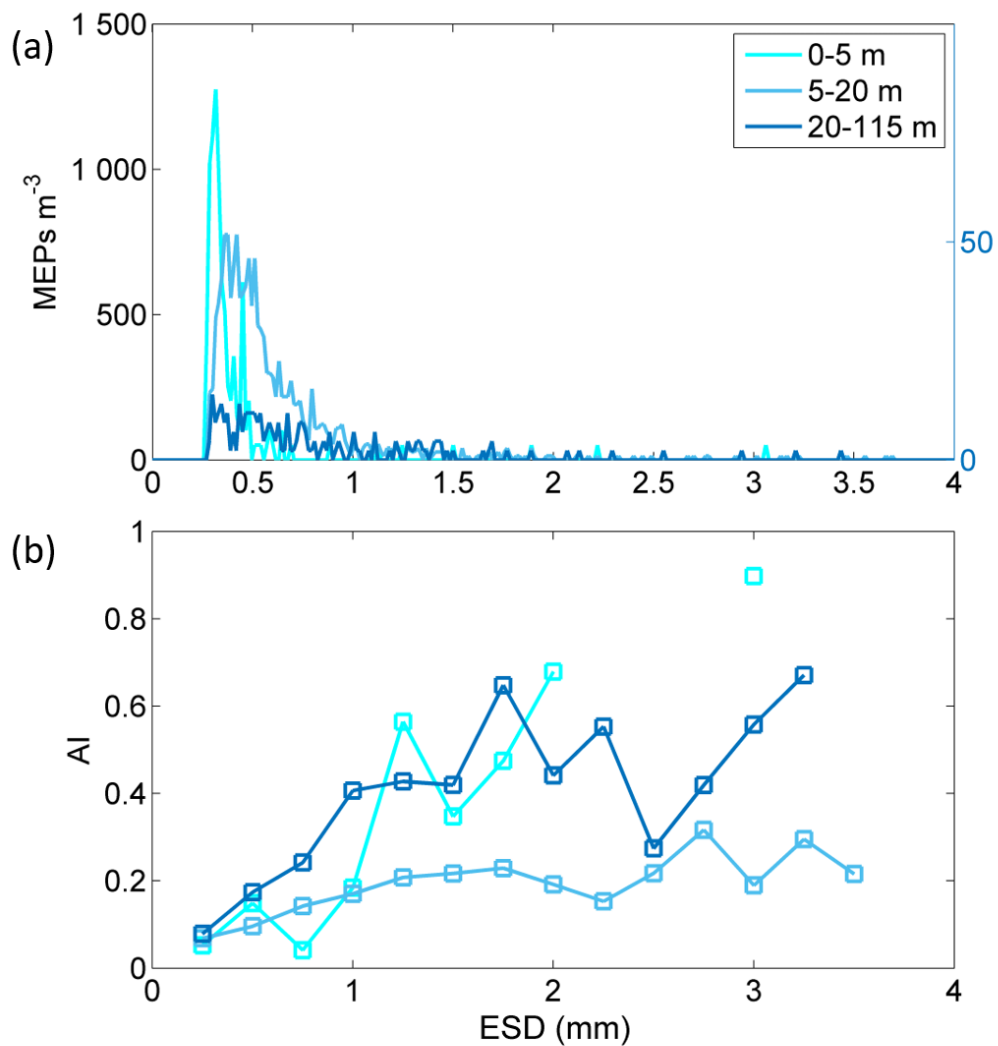


Fig. 6. (a) Size spectra of MEPs and (b) mean attenuation index (AI) as a function of the MEP size (0.1 mm interval) at station C (see Fig. 2, 4 & 5) in 3 different water layers. Because of lower values, MEP abundances for the deepest layer (20-115 m) is displayed on a separate axis (right).

Table 1. Kruskal-Wallis test applied on the percentage of detritus, % of MEPs and AI considering as factors the 3 habitats defined in Espinasse et al. 2014. Post-hoc results are also shown.

Parameter	X^2	p-value	Post-hoc			
%detritus	25.88	$2.39 \cdot 10^{-6}$	Habitat #1	Habitat #2	H2 > H1;	
			Habitat #2	<0.001	-	H2 > H3
			Habitat #3	n.s.	<0.001	
%MEPs	39.09	$3.23 \cdot 10^{-9}$	Habitat #1	Habitat #2	H2 > H1;	
			Habitat #2	<0.001	-	H2 > H3
			Habitat #3	n.s.	<0.001	
AI	61.85	$3.7 \cdot 10^{-14}$	Habitat #1	Habitat #2	H3 > H1;	
			Habitat #2	n.s.	-	H3 > H2
			Habitat #3	<0.001	<0.001	

Table 2. Summary describing how to interpret the LOPC abundance with the help of the two indicators, %MEPs and AI, and typical situations leading to these indicator values.

	Low AI (< 0.2)	High AI (> 0.2)
High % of MEPs (> 2) (> 5 overestimation)	Aggregate formation if stratified waters, can be promoted by high primary production	High concentration of big copepods (> 1.5 mm), mainly in high latitude areas, or terrestrial input (sand)
Low % of MEPs (< 2)	Low detritus, if high chl-a concentration, phytoplankton chains or colonies characterized by small MEP size (< 400 μm ESD)	Clear water, LOPC mainly counting zooplankton

Table 3. Comparison of particle characteristics in different regions and different environmental conditions. Only stations deeper than 50 m were included. High chl-a: max chl-a > 1 mg m⁻³.

Environmental conditions	Region / remarks	# part m ⁻³ min-max nbr. of stn.	AI mean (min-max)	%MEPs mean (min-max)	References
Mixed waters	Antarctic Peninsula – Continental bay Clear water and few large-sized organisms	3600 – 36200 <i>n=16</i>	0.24 (0.09 – 0.54)	0.34 (0.16 – 1.61)	Espinasse et al. 2012
	Svalbard – Cross shelf section	2000 – 26000 <i>n=10</i>	0.48 (0.36 – 0.56)	0.33 (0.14 – 2.17)	Basedow Unpublished data
	North Atlantic – Open ocean Very clear water	4000 – 6000 <i>n=3</i>	0.46 (0.31 – 0.62)	0.76 (0.70 – 0.85)	Basedow et al. 2016
	Brazil coast – Continental slope	6900 – 146000 <i>n=37</i>	0.22 (0.13 – 0.3)	0.87 (0.54 – 2.04)	Schultes and Lopes 2009
	NW Mediterranean Sea – Continental slope	18000 – 30000 <i>n=43</i>	0.25 (0.11 – 0.44)	0.90 (0.40 – 1.92)	This study
	Polar fjord – Outer part high chl-a	130000 – 240000 <i>n=2</i>	0.10 (0.08 – 0.11)	1.16 (0.71 – 1.61)	Trudnowska et al. 2014
Stratified waters	Polar fjord – Glacier area Input of particles from melt-water discharge	475000 – 865000 <i>n=4</i>	0.08 (0.07 – 0.08)	3.90 (2.27 – 6.25)	Trudnowska et al. 2014
	NW Mediterranean Sea - Continental shelf	48000 – 70000 <i>n=8</i>	0.15 (0.11 – 0.22)	2.08 (1.13– 4.01)	This study
Stratified waters + high chl-a	NW Mediterranean Sea - Freshwater run-off	100000 – 215000 <i>n=13</i>	0.12 (0.07 – 0.14)	3.21 (1.70 – 5.36)	This study

Highlights

- A new method to interpret LOPC counts was developed.
- The environmental conditions and the mechanisms resulting in detritus formation were identified.
- LOPC derived indicators were used successfully to determine the contribution of detritus in total counts.
- Thresholds for these LOPC indicators are used to define different situations with varying contribution of detritus.
- The method was applied to worldwide dataset and showed consistent results.